

- ²⁰C. J. Duthler and G. L. Pollack, Phys. Letters 31A, 390 (1970).
²¹R. F. Harris-Lowe, C. F. Mate, K. L. McCloud, and J. G. Daunt, Phys. Letters 20, 126 (1966).
²²D. J. Martin and K. Mendelssohn, Phys. Letters 30A, 107 (1969).
²³W. E. Keller and E. F. Hammel, Physics 2, 221 (1966).
²⁴H. A. Notarys, Phys. Rev. Letters 22, 1240 (1969).
²⁵J. S. Langer and M. E. Fisher, Phys. Rev. Letters 19, 560 (1967).
²⁶W. E. Keller and E. F. Hammel, Phys. Rev. Let-
17, 998 (1966).
²⁷R. J. Donnelly, Phys. Rev. Letters 14, 939 (1965).
²⁸W. M. van Alphen, G. J. Van Haasteren, R. De
Bruyn Ouboter, and K. W. Taconis, Phys. Letters 20,
474 (1966).
²⁹C. J. Duthler and G. L. Pollack, Bull. Am. Phys.
Soc. 13, 912 (1968); 14, 96 (1969).
³⁰J. F. Allen and C. C. Matheson, Proc. Roy. Soc.
(London) A290, 1 (1966).
³¹J. Wilks, in Ref. 6, p. 416.

PHYSICAL REVIEW A

VOLUME 3, NUMBER 1

JANUARY 1971

Cross Sections for Electron Capture and Loss by Fast Bromine and Iodine Ions Traversing Light Gases*

Hans D. Betz

Massachusetts Institute of Technology, Cambridge, Massachusetts 02139

and

G. Ryding and A. B. Wittkower

High Voltage Engineering Corporation, Burlington, Massachusetts 01803

(Received 17 August 1970)

Bromine and iodine ions, accelerated to energies between 6 and 15 MeV, were passed through thin gas targets of H₂ and He. Nonequilibrium charge distributions were measured, from which cross sections for capture and loss of one or more electrons by the heavy ions were determined by means of a least-squares fitting technique. The cross sections are discussed with regard to their functional dependence on the charge and velocity of the ions. Owing to the unprecedented precision of the results, characteristic irregularities were revealed in the charge dependence of the cross sections for both capture and loss of one and two electrons. These effects are attributed to the influence of shell structure and residual excitation of the ions.

I. INTRODUCTION

Atomic collisions between energetic ions and matter have been studied for a number of years, both for the purpose of understanding the fundamental physics of atomic interactions and for a more practical reason, the necessity of producing intense high-energy beams from heavy-ion accelerators. In the past, the lighter ions have been studied intensively.¹ Since only a few measurements have been reported²⁻⁶ of charge-exchange cross sections for ions with a nuclear charge greater than 18, additional investigations are of the greatest importance. For example, systems of highly accurate cross sections for the capture and loss of one or more electrons in a single collision by fast heavy ions with many adjacent charge states have never been reported in detail. Although it is believed that existing theories describe the essentials of the charge-changing mechanisms, it is not yet possible to predict values, often as large as 10⁻¹⁵ cm², of the many cross sections involved in the interaction.

In this experiment, Br and I ions have been accelerated to energies between 6 and 15 MeV, passed through targets of He and H₂ gas of varying thick-

ness, and the distributions of ionic charge states in the emerging beam were detected. The experimental procedure⁷ has been described previously, as well as the technique of analysis^{6,8} which has been employed to obtain charge-changing cross sections with uncertainties of 5 to 10%. Additional details of both the experimental procedure and the data treatment, which yielded these high accuracies, are included in the body of this paper. Results confirm the existence of shell effects previously reported,⁶ but a thorough analysis of the data showed that these shell effects can be strongly influenced by ions which are in excited states before the charge-changing collisions occur. This indicates that residual ion excitation is of greater importance than previously believed and cannot be neglected in many heavy-ion experiments. A method of analysis is discussed to take into account residual ion excitation in order to obtain consistent sets of charge-changing cross sections.

In the present investigation, shell structures were identified in the double-capture cross sections, as well as in the single- and multiple-loss cross sections. The shell effects in electron-loss probabilities are small and seem to support qualitative theoretical assumptions about single electron loss.

Very large probabilities were found for multiple electron loss in single collisions with He atoms, a result which raises interesting questions about the mechanism of multiple electron loss in light targets. Though only three different energies were investigated for Br and I ions, maxima in the velocity dependence of the loss cross sections are indicated at characteristic ion velocities, in approximate agreement with theoretical expectations.

II. EXPERIMENTAL PROCEDURE

The apparatus used in the present experiment (Fig. 1) has been described in detail.⁷ Therefore, only those features of the experimental procedure and data-analysis technique are given here which are essential for an understanding of the accuracy of the final results.

A. Incident Charge States

The accelerator system, which included electrostatic and magnetic analysis, delivered a monoenergetic beam of ions in a single charge state q_a . This beam was directed into a charge converter cell (CV) (Fig. 1) to produce ions of different charge states q_0 . An electrostatic deflector (ED) selected ions with the desired incident charge, which were passed on to the target cell. The ranges of incident charge states q_0 , which are listed in Table I, were limited by the intensity of the ion beam and the deflection power of ED. In those cases where $q_0 = q_a$, no gas was admitted into CV and the good vacuum in the beam line ($P \leq 10^{-6}$ Torr) allowed a major fraction of ions to reach the target cell without having suffered any charge-changing collisions between the accelerator and the target. Since the corresponding time of flight for these ions always exceeded 2×10^{-6} sec, it was justified to assume that essentially all residual excitation was dissipated upon arrival at the target cell. These cases will be of importance in connection with lifetime estimates for excited ions.

B. Target Cell

The target cell consisted of a differentially pumped system with an effective inner length of 3.65 cm. Pressures P of the target gas between 0 and 2 Torr could be maintained. The pressures

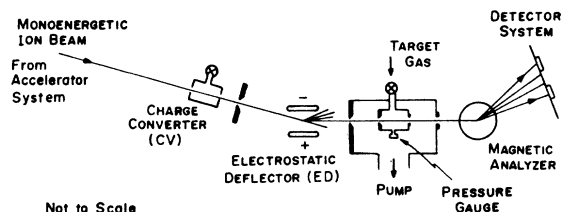


FIG. 1. Experimental apparatus.

TABLE I. List of the experimental parameters; q_a and q_0 denote the ionic charge states obtained from the accelerator and the charge converter, respectively. All values of q_0 from the listed ranges were used as incident charge states.

Ion	q_a	Energy (MeV)	Target	q_0
Br	3 +	6	He	2-9
	5 +	10	He	3-10
	7 +	14	He	4-10
	6 +	14	H ₂	4-8
I	3 +	6	He	2-9
	5 +	10	He	3-9
	7 +	15	He	4-10

were measured with a differential manometer which allowed an accuracy of better than about 3% for $P \geq 3 \times 10^{-4}$ Torr. During all runs, P was kept constant within 1%. When larger drifts of P occurred, the system was allowed to settle and the run was restarted.

Generally, P was varied from 0 to 2×10^{-3} Torr in about five steps, but in a few cases as many as 25 steps were taken up to 2 Torr. For the system used in these experiments, the target thickness π was related to the pressure of the target gas by

$$\pi = 1.23 \times 10^{17} P \text{ molecules/cm}^2, \quad (1)$$

where P is given in Torr. The amount of residual gas in the system was so small that charge exchange due to gases other than the target gas occurred on the average to only 0.3%, but never to more than 2% of the incident ions. As an example, Fig. 2 shows charge-state distributions for incident Br^{4+} at 14 MeV and I^{2+} at 6 MeV, obtained in the absence of target gas. The attenuation of the incident beams amounts to 0.16% and 0.51%, respectively.

C. Detection

The charge components of the ion beam emerging from the target cell were separated magnetically and detected individually with surface-barrier counters. Two components were always measured simultaneously in order to eliminate the effects of beam intensity fluctuations and to obtain the relative intensities of each charge fraction. Since one component of each pair was always allowed to accumulate to a total of greater than 10^5 counts, the smallest significant fractions accumulated to a total of approximately 100 counts, thereby enabling a measurement to be made with a statistical error of less than 10%. The actual counts were used as input data for the computer program with which the cross-section analysis was performed.

Special care was given to the distributions obtained in the absence of target gas for the various incident charge states (Fig. 2). Since these distri-

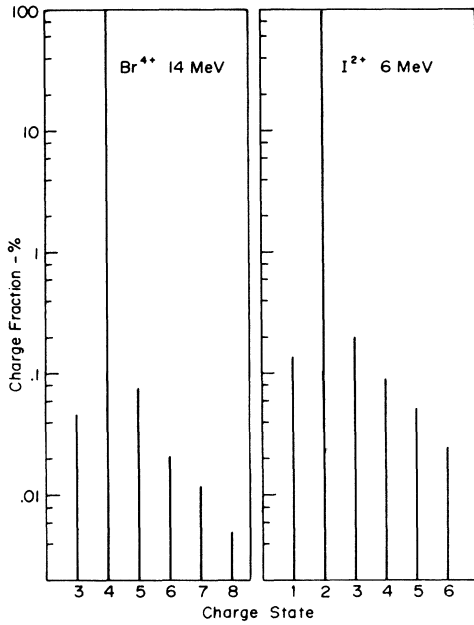


FIG. 2. Charge-state distributions for incident Br^{4+} ions at 14 MeV and I^{2+} ions at 6 MeV, obtained in the absence of target gas.

butions were not fitted but used as initial conditions in the final numerical analysis, it was desirable to keep these errors particularly small.

Two experimental nonequilibrium charge distributions are shown in Figs. 3(a) and 3(b) for 14-MeV Br ions with incident charge states $7+$ and $8+$, stripped in H_2 and He, respectively. Because of the logarithmic scale for the target thickness π , the charge fractions obtained for $P=0$ in the absence of target gas are indicated separately on the left. The solid lines represent the fit which is described in Sec. III. It can be seen from Fig. 3 that the data points are not greatly scattered and that statistical errors become noticeable only for charge fractions smaller than about 0.1%.

III. DATA TREATMENT AND ANALYSIS

A. Mathematical Background

Experimental nonequilibrium distributions were used to determine a large number of charge-changing cross sections $\sigma(q, q')$, where q and q' denote the ionic charge before and after a charge-changing collision. Assuming that a single set of constant cross sections governs the charge-changing processes, the dependence of the charge fractions F_q on the target thickness can be described by a well-known system of differential equations:

$$\frac{d}{d\pi} F_q(\pi) = \sum_{q' \neq q} q' [\sigma(q', q) F_{q'} - \sigma(q, q') F_q], \quad (2)$$

where π and σ are given in units of molecules/ cm^2 and $\text{cm}^2/\text{molecule}$, respectively. In experiments

with very light projectiles (like H or He), or for heavier particles at very low energies (keV range), where only two or three different charge states are important, simple analytical solutions for $F_q(\pi)$ can be derived from Eq. (2).⁹ However, this is hardly feasible for fast heavy ions, where a much larger number of charge states become important, and where the number of relevant charge-changing cross sections increases sharply.

Among the analytical solutions of Eq. (2) which have been suggested,^{1,9} most frequent use has been made of a linear approximation, $F_{q0}(\pi) = \pi\sigma(q_0, q')$, which is expected to hold for sufficiently small values of π . It can be seen from Fig. 3, however, that this condition is extremely difficult to realize in practice and that small charge components generally do not increase linearly with the target thickness.

In the present work, a least-squares technique (FIT) was employed, the mathematical principle of which has been recently described.^{6,8} The cross sections were determined with FIT so that the charge fractions computed from the complete system of Eq. (2) reproduced best the experimental fractions in a least-squares sense. The FIT procedure can be applied directly to any number of experimental nonequilibrium charge distributions in any pressure range, provided that Eq. (2) is valid for the experimental system under consideration. In order to determine the uncertainties of the cross sections, appropriate errors $\delta F'$ of the experimental fractions were introduced into FIT.

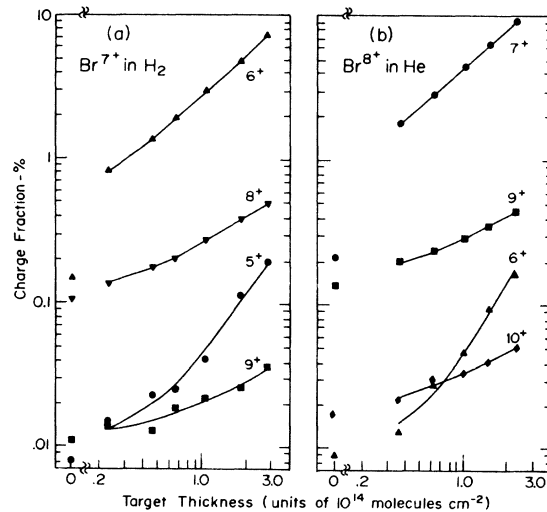


FIG. 3. Nonequilibrium charge distributions for 14-MeV Br ions in hydrogen (a) and helium (b). All incident fractions with charge $7+$ and $8+$, respectively, are not displayed. The solid lines are obtained from the fit with the final cross sections and originate, in the analysis, from the data points at target thickness zero.

Due to uncertainties in the measurement of the target thickness, the effective errors δF were chosen larger than the mere statistical errors which can be derived from the count rates for the individual charge fractions.

B. Selection and Correlation of Cross Sections

For a given data set, it is not always obvious how many cross sections one should include in Eq. (2). Some cross sections σ_μ may have very little influence on the charge distributions so that the data will not permit a determination of these cross sections with errors $\delta\sigma_\mu$ which are reasonably small ($\delta\sigma_\mu/\sigma_\mu \lesssim 100\%$). If σ_μ , nevertheless, is used as a variable in FIT, it may assume unreasonable values within a wide range limited by $\pm\delta\sigma_\mu$. If the data lead to a strong correlation between the values of σ_μ and another cross section σ , which is determined with good accuracy, an unreasonable σ_μ may strongly affect the results for both σ and $\delta\sigma$. This distortion is avoided by eliminating σ_μ as a variable from FIT: σ_μ is assigned either the value zero or a reasonable fixed value suggested by the general trend of the cross sections which are determined with greater accuracy. Mathematically, the two possibilities are equally useful, though the latter one may be preferred for physical reasons. It is necessary, however, to include all those cross sections as variables into FIT which have small errors and are correlated strongly to each other.

The proper selection of those cross sections to be used is easily performed in a test FIT, in which all possible cross sections are taken as variables. The resulting errors $\delta\sigma$ can be used to decide whether a cross section must be kept as a variable in the final FIT.

As an example, consider the data illustrated in Fig. 3(a). In the entire range of pressures, the incident charge fraction Br^{7+} (which is not shown in Fig. 3) drops from 99.7 to 92.1%. This decrease is essentially due to single collisions, which populate the charge states 5+, 6+, 8+, and 9+. One

might expect, therefore, that the only important cross sections are $\sigma(7, q')$ where $q' = 5, 6, 8$, and 9. A test FIT shows, however, that the capture cross section $\sigma(6, 5)$ can also be determined with small error and must, therefore, be included into FIT. In Table II, these particular cross sections are listed together with their errors and correlation coefficients. In that example, only $\sigma(7, 5)$ and $\sigma(6, 5)$ are strongly correlated. As a consequence, if $\sigma(6, 5)$ were neglected, the double-capture cross section $\sigma(7, 5)$ would change from its best value $1.6 \times 10^{-18} \text{ cm}^2$ by more than 100% to the unjustified value of $3.8 \times 10^{-18} \text{ cm}^2$.

C. Cross-Section Analysis under the Influence of Residual Ion Excitation

It was found from apparent inconsistencies in preliminary fits that in the present experiment residual ion excitation could not be neglected. The length of the target cell was not the only reason, since most cross sections were determined from data taken at pressures below 2×10^{-3} Torr and only few ions had more than one collision within the target cell. Apparently, excited ions with lifetimes longer than those previously anticipated were responsible for the observed effects.

When the lifetimes of excited ions are longer than or comparable with the average time between two successive charge-changing collisions, a proper description of the processes requires the addition of cross sections for excited states. This problem is particularly difficult when charge fractions contain varying amounts of ground and excited states. Fortunately, the present data could be analyzed by a more complicated procedure so that separate cross sections could be obtained for the ions in a particular charge state, either in the ground state or as a sum of excited states. This is achieved if each nonequilibrium distribution is analyzed individually in the range of target thicknesses where single collisions predominate, i. e., distributions which belong in the absence of residual excitation to the same set of cross sections can no longer be analyzed simultaneously in FIT. Instead of only seven fits (Table I), now 50 fits became necessary, one for each of the measured nonequilibrium charge distributions. This procedure ensured that in each FIT a particular cross section entered with only a single value which, of course, may lie anywhere between the values for ground and fully excited states.

The data shown in Fig. 3(a), for example, give the cross section $\sigma(7, 6)$ for the ground state, because the incident Br^{7+} ions ($q_0 = q_a$) traveled a sufficiently long path ($\sim 10^3 \text{ cm}$) to allow radiative de-excitation before entering the target cell. In contrast, the value obtained for $\sigma(6, 5)$ from the same data set (Table II) reflects added contributions from excited states. Nearly all ions with charge 6+ have

TABLE II. Correlation coefficients for the five cross sections $\sigma_{q-q'}$ which are used to describe the nonequilibrium charge distribution obtained for 14-MeV Br^{7+} ions stripped in H_2 gas [see Fig. 3 (a)]. The cross sections and their uncertainties $\delta\sigma_{q-q'}$ are given in units of $10^{-16} \text{ cm}^2/\text{molecule}$.

$q \rightarrow q'$	6 \rightarrow 5	7 \rightarrow 6	7 \rightarrow 5	7 \rightarrow 8	7 \rightarrow 9
7 \rightarrow 6	-0.042				
7 \rightarrow 5	-0.848	-0.066			
7 \rightarrow 8	0.002	-0.010	0.000		
7 \rightarrow 9	0.000	0.003	0.000	-0.016	
$\sigma_{q-q'}$	1.40	2.74	0.016	0.162	0.010
$\delta\sigma_{q-q'}$	0.282	0.075	0.006	0.012	0.001

been formed inside the target cell by electron capture, often into excited states. If the related lifetimes are long enough, those ions of charge $6+$ which pick up another electron in the target cell may still be substantially excited when that second collision, $6+ \rightarrow 5+$, occurs. This explains why the resulting cross section $\sigma(6, 5) = 1.4 \times 10^{-16} \text{ cm}^2$ (Table II) differs substantially from and is lower than $\sigma(6, 5) = 2.66 \times 10^{-16} \text{ cm}^2$ (Table III), which is obtained from a separate FIT of a nonequilibrium distribution where Br^{6+} ions were incident in states with an average excitation close to zero.

In this paper, the cross sections closest to the ground state will be reported, although most numerical fits also yielded cross sections for capture and loss from excited states. A separate publication will be devoted to the rather complicated excitation effects and the related radiative lifetimes.

IV. RESULTS

All of the 50 nonequilibrium charge distributions (see Table I), for which Fig. 3 gives two examples, have been analyzed separately by means of the technique described in the Sec. III. Table III lists all the resulting cross sections $\sigma(q, q+n)$ in units of $10^{-16} \text{ cm}^2/\text{molecule}$ and their most probable errors $\delta\sigma/\sigma$ in percent for the loss of one to four electrons and the capture of one and two electrons, corresponding to $n = 1, 2, 3, 4$, and $n = -1, -2$, respectively. As can be seen from Table III, most cross sections were obtained with good accuracy; systematic errors are not included. The only exceptions are the double-capture cross sections $\sigma(q, q-2)$, which have on the average an uncertainty of about 50%. This must be expected because the

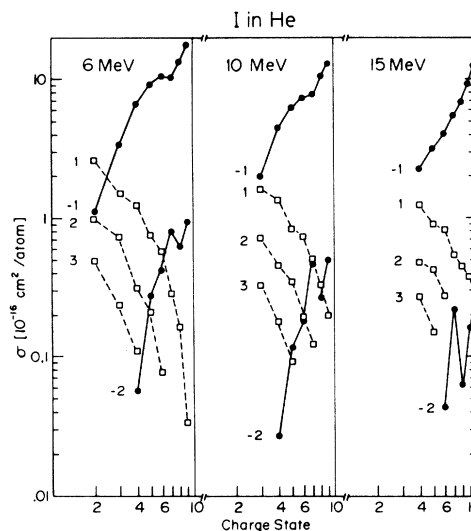


FIG. 5. Cross sections for electron capture (solid lines) and loss (dashed lines) by I ions in helium gas as a function of the initial ionic charge state.

growth rate of charge fractions F_{q-2} was dominated by single capture $\sigma(q-1, q-2)F_{q-1}$, rather than by direct double capture, $\sigma(q, q-2)F_q$. The double-capture cross sections, therefore, have only a small influence on the nonequilibrium distributions and this is reflected in increased errors.

Since multiple-loss cross sections are large compared with multiple capture, they could be determined with better accuracy even in the cases $n = 3$. To complement the discussion, some of the cross-section results are displayed in Figs. 4-7.

For the majority of those cross sections obtained

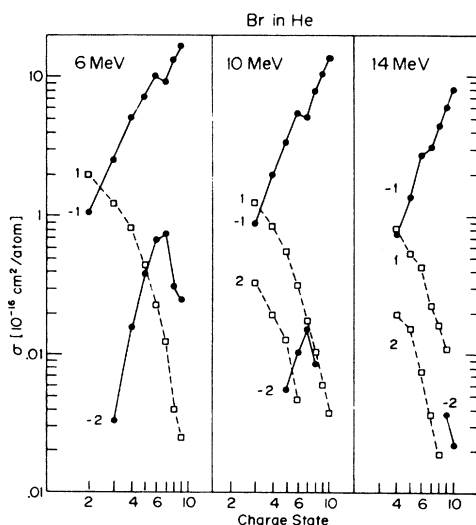


FIG. 4. Cross sections for electron capture (solid lines) and loss (dashed lines) by Br ions in He gas as a function of the initial ionic charge state.

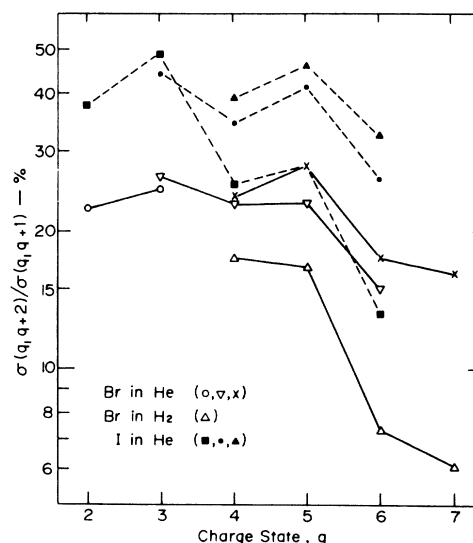


FIG. 6. Ratios of cross sections for double- and single-electron loss by Br and I ions in H_2 and He gas as a function of the initial ionic charge state.

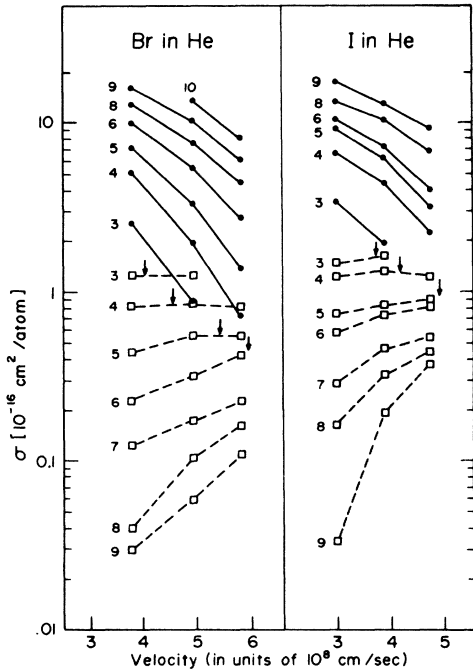


FIG. 7. Velocity dependence of the cross sections for single-electron capture (solid lines) and loss (dashed lines) by Br and I ions in He.

in He, Figs. 4 and 5 show the dependence as a function of the ionic charge on a log-log scale for Br ions at 6, 10, and 14 MeV and for I ions at 6, 10, and 15 MeV. The solid and dashed lines refer to capture ($n = -1, -2$) and loss ($n = 1, 2, 3$), respectively. Error bars are omitted from the graphs because the uncertainties are listed in Table III. Figure 6 shows the ratio of double loss to single loss, $\sigma(q, q+2)/\sigma(q, q+1)$, as a function of the initial charge q in the range $q = 2-7$. In Fig. 7, the cross sections for single capture (solid lines) and loss (dashed lines) of Br and I ions stripped in He are plotted on a logarithmic scale versus the ion velocity. Initial charge states are identified by the numbers close to each curve. Because of the pronounced shell effects in $\sigma(7, 6)$, these cross sections were omitted from the graph. For some loss cross sections, arrows indicate ion velocities, close to the maximum cross-section values, which are discussed in Sec. V.

V. DISCUSSION

A. Single-Capture Cross Sections

The probability $\sigma_c(q)$ for an ion of charge q to capture an electron from the target atoms during an encounter generally increases with q . At charge state 7+, however, discontinuities were found. In most cases, the cross section $\sigma_c(7)$ was unexpectedly small, sometimes even below $\sigma_c(6)$. Similar small values of $\sigma_c(7)$ for Br ions have first been reported in a recent publication⁶ and have been at-

tributed to shell effects. Both Br and I ions of charge 7+ are in configurations of closed shells and capture of an electron will take place only into a new shell, the N and O shell, respectively. It may therefore be expected that the probability for such a capture process could be significantly reduced. Though the present results are not in qualitative contradiction to this conclusion, it is now clear that this interpretation of the observed shell effects was oversimplified and that it is necessary to take into account residual ion excitation. In fact, the state of excitation of a capturing ion may affect the measured capture cross sections to a greater extent than direct shell effects in the absence of excitation. In some cases, residual excitation of an ion after capture of a first electron can effectively decrease the capture probability for a second electron by a factor of 2 or 3 as in the example discussed above. Apparently, the lifetimes of excited Br and I ions with charge states within the range investigated here are often long enough that residual excitation by previous collisions influences many of the present electron-capture cross-section values.

For 14-MeV Br and 15-MeV I, the incident ions of charge $q_a = 7$ have been formed in the terminal of the accelerator (Table I) and during the 10-m flight to the target cell, most residual excitation would have been dissipated. These measured values $\sigma_c(7)$, therefore, should be dominated by capture of ground-state ions. It can be seen from Figs. 4 and 5 that in these two cases the decrease of $\sigma_c(7)$ is much less pronounced—practically absent for I. In the cases when the incident charge q_0 was different from q_a (Table I), q_0 was produced at a distance l of about 53 cm in front of the target cell. These capture cross sections $\sigma_c(q_0)$ may contain an excitation effect whenever the condition $\tau v \geq l$ is fulfilled, where τ is the relevant lifetime of the excited state and v denotes the ion velocity. Presently, not enough is known about the lifetimes involved to enable the difference of our capture cross sections from the true ground-state values to be estimated. It seems, however, that these differences are fairly small, because the cross sections $\sigma_c(q_0 = q_a)$ do not differ from the general trend for $q_a < 7$ (and for $q_0 > 8$ the lifetimes are expected to be so short that any residual excitation should have been dissipated by radiation within the mean collision time).

It is important to note that the loss cross sections under investigation do not noticeably depend on the residual excitation discussed above. This somewhat surprising result has been discussed in two recent publications^{10,11} and will be dealt with in detail in a forthcoming paper.¹²

Several attempts have been made previously to approximate the capture cross sections in the form

$$\sigma_c(q) = f(v)q^\alpha, \quad (3)$$

where α was assumed to be independent of the ion velocity v . For charge states close to the mean ionic equilibrium charge \bar{q} , our results indicate values of α between 2 and 3. We show below, however, that the exponent α is likely to increase significantly with the ion velocity. If both capture and loss cross sections are approximated by the form of Eq. (3) (see Ref. 13), the use of constant exponents, which was first suggested by Bohr,¹³ leads to an increase of the width Γ of the equilibrium charge distribution with increasing mean charge $\bar{q}(v)$, $\Gamma \propto \bar{q}(v)^{1/2}$. Such an increase of Γ has not been found over a wide range of velocity, including the velocities of typical fission fragments. A thorough analysis of this aspect, beyond the scope of the present paper, leads one to the conclusion that, in order to match the experimental widths, either $\sigma_c(q)$ or $\sigma_l(q)$ or both vary with the velocity in a manner such that α will not remain a constant value. This appears to be supported by the present and other data^{2,6} which were obtained in a wide velocity range; for a given ion species, α in Eq. (3) increases when \bar{q} increases if it is derived from a smoothed curve in the range of charge states close to \bar{q} , which essentially determine the equilibrium distribution.

For most charge states, our capture cross sections for Br and I ions do not always coincide well when interpolated for equal ion velocities. This appears to be a further consequence of the dependence of α on the mean charge. In the approximation equation (3), the variation of α with \bar{q} implicitly introduces a slight dependence on the nuclear charge Z of the ions because \bar{q} is a function not only of v but also of Z . This leads to an important conclusion: One has to abandon the hypothesis that electron-capture probabilities depend only on the charge of the capturing ion, but not – apart from shell effects – on the nuclear charge of the ions.^{13,14} Instead, it may be concluded that capture cross sections for different ion species at the same ion velocity are not necessarily identical for charge states in the vicinity of \bar{q} . Although these differences are not likely to be very pronounced especially for ions with similar nuclear charge, they represent a basic factor in the theoretical understanding of electron capture by heavy ions.

It is clear from Fig. 7 that the capture cross sections decrease rapidly with increasing ion velocity. For all charge states there is a rather sharp maximum at small velocities outside the range of this investigation. Since our values lie too close to that maximum, no attempt has been made to express $\sigma_c(v)$ by means of a simple power law. This appears to be feasible only at higher ion velocities.¹

B. Double Capture

In He targets, the probability for simultaneous

capture of two target electrons in a single encounter is very small and ranges typically from 1 to 5% of the capture for one electron. Though the uncertainties in these cross sections are generally large, it is possible to find not only a strong increase of double capture with increasing charge state, but also a shell effect which is just outside the error limits. In all cases, $\sigma(8, 6)$ is smaller than $\sigma(7, 5)$. It is interesting to note that this shell effect occurs for ions of charge 8+ rather than 7+. This will happen only if one assumes that the probability for capture depends partly on the final state. For Br and I ions, charge state 6+ is apparently a state which is less likely than adjacent charge states. Thus, the shell effects discussed above for single capture, which reduce the probability $\sigma(7, 6)$, also cause a reduction of $\sigma(8, 6)$. In judging the magnitude of this shell effect, one again has to take into account the possibility of residual ion excitation. It is not obvious to what extent the effect will be found in ground-state cross sections and how much influence must be attributed to residual excitation of the capturing ions. Still, for I at 15 MeV, the incident ions of charge 8+ were in the ground state (Table I) and the shell effect is clearly visible.

The cross sections for single capture in H₂ and He targets reported in Table III do not differ by more than 15% if given in cm²/molecule. Double capture is very unlikely in H₂; for Br at 14 MeV, the experimental ratios $\sigma(q, q-2)/\sigma(q, q-1)$ were always below 0.01. A shell effect similar to the one found in He targets may also exist in H₂, but our data are too limited to draw further conclusions.

C. Single and Multiple Loss

The probability for loss of electrons as a consequence of collisions with target atoms decreases with the charge state of the ions. For Br, stripped in He, this decrease is rather smooth (Fig. 4) but steeper for the higher charge states. For I ions, stripped in He, the general trend is similar, but a step structure is revealed which, though weak, is clearly outside the experimental errors (Fig. 5). At all energies, the single-loss cross sections from charge states 4+ and 6+ are somewhat larger than a smoothed trend would suggest. As charge states 4+ and 6+ correspond to an electronic structure in which one electron is retained outside a closed subshell (4s) and a closed shell (3d), it is likely that the relative increase in the probability is caused by the removal of such an electron. Interestingly, a similar effect is visible in the double-loss cross sections. As one would expect considering the final states involved, the larger cross sections now occur at charge states 3+ and 5+.

These shell effects are not very strongly pronounced and could be found only because the experimental errors were generally as small as 5%.

Nevertheless, the existence of such effects and their magnitude allows some conclusions to be drawn about the mechanism of electron loss. Although the ionization energies of the most loosely bound electrons in 6+ and 7+ Br and I ions differ by almost a factor of 2, the loss cross sections do not appear to be greatly affected. This result, as well as the smallness of the observed shell effect, can be explained only if one assumes that the most loosely bound electron contributes a small but non-negligible part to the measured single-loss cross sections, and that other electrons in the ion also have a substantial probability of being removed in a collision. Clearly, these contributing electrons are not confined to the outermost subshell or shell; therefore, shell effects will be diluted and are difficult to observe. This general reasoning is also in agreement with conclusions derived from the density effect for heavy ions.¹⁰⁻¹²

In Bohr's theory of electron loss,¹³ as well as in further theoretical investigations,^{1,14} loss cross sections contain a summation over many electrons in an ion. However, the many simplifications used in these models did not allow a reliable estimate of the relative contributions of the individual electrons. At least, in the original explanation of the density effect,¹³ which was shown to be partly incorrect,¹¹ the contributions of the electrons other than the most weakly bound one have been grossly underestimated. It is now evident that inner-shell electrons cannot be neglected in charge-changing collisions with even very light targets, though in these cases the spatial overlap of the electron wave functions of ion and target is rather small.

An improved description has been achieved for medium mass ions, if one assumes that within a shell the cross sections for single loss vary approximately proportionally to the number of electrons q_s in their outer shell.¹ Though this assumption works quite well in some cases, it is generally a crude approximation for heavy ions and light targets. Our conclusions above make it clear that q_s is not always easy to define because other electrons than those in the outer shell must be considered. Furthermore, the suggested proportionality to q_s is disturbed because the binding energy of a particular electron changes significantly when many outer electrons are removed.

The simultaneous loss of two electrons due to single encounters with He atoms occurs with quite large relative probabilities and may reach almost

50% of the single-loss cross section. The ratios $\sigma(q, q+2)/\sigma(q, q+1)$ generally decrease with increasing q , but at charge states 3+ and 5+ maxima occur (Fig. 6), which are due to the shell effects discussed above. Here, these effects are more pronounced, because the plotted ratios combine relatively large values of the double loss with relatively small values of the single loss and vice versa. As a consequence, the shell effects are now also visible for Br ions. The somewhat stronger binding of electrons in Br ions compared to I ions of the same charge is probably part of the reason why the double-loss cross sections are smaller in Br than in I ions.

Cross sections for single loss in a H₂ target are substantially smaller than in He. The relative cross sections for loss of three and four electrons decrease rapidly and amount to 18.9 and 5.9% for 6-MeV I in He, but only to 3.65 and 0.54% for 14-MeV Vr in H₂, respectively.

The loss cross sections increase with the ion velocity until a maximum is reached at a characteristic velocity v_q and then decrease slowly for higher ion velocities. In a first-order approximation, v_q is expected to be equal to the velocity u_q of the most loosely bound electron in the ion of charge q given by¹

$$u_q = (2I_q/m)^{1/2}, \quad (4)$$

where I_q is the ionization potential of the electron being removed and m is the electron mass. Although our data cover only a small velocity range, Fig. 7 clearly indicates the maxima and their shift to higher velocities for increasing q . For the loss cross-section curves $\sigma_q(v)$, which show or come close to the maximum, the velocities u_q , computed from Eq. 4, are indicated by arrows close to these curves. It is obvious that u_q is indeed close to the true maximum at v_q . Our limited data and the broad maxima do not allow us to determine a correction factor γ , defined by $v_q = \gamma u_q$, but the value of $\gamma = 1.3$, which has been estimated from other data for He targets,¹ is probably too large at least for charge states 3+ to 5+ for Br and I ions in the present investigation.

It can be understood that v_q should be somewhat larger than u_q , because inner electrons which are more strongly bound and have higher orbital velocities also contribute to single loss. The double-loss cross sections show a behavior similar to the cross sections for single loss, but the maxima appear to be shifted slightly more towards higher velocities.

*Work supported in part through funds provided by the U.S. Atomic Energy Commission Contract No. AT(30-1)-2098.

¹Electron capture and loss by fast ions ($Z \leq 18$) has been reviewed by V. S. Nikolaev, Usp. Fiz. Nauk **85**, 679 (1965) [Soviet Phys. Usp. **8**, 269 (1965)].

²N. Angert, B. Franzke, A. Möller, and Ch. Schmelzer, Phys. Letters **27A**, 28 (1968).

³A. Möller, N. Angert, B. Franzke, and Ch. Schmelzer, Phys. Letters **27A**, 621 (1968).

⁴G. Ryding, A. B. Wittkower, and P. H. Rose, Phys. Rev. **184**, 93 (1969).

⁵G. Ryding, A. B. Wittkower, G. Nussbaum, A. Saxmann, R. Bastide, Q. Kessel, and P. H. Rose, *Phys. Rev. A*, **1**, 1081 (1970).

⁶S. Datz, H. O. Lutz, L. B. Bridwell, C. D. Moak, H. D. Betz, and L. D. Ellsworth, *Phys. Rev. A*, **2**, 430 (1970).

⁷G. Ryding, A. B. Wittkower, and P. H. Rose, *Phys. Rev.* **185**, 129 (1969).

⁸H. D. Betz, *Bull. Am. Phys. Soc.* **14**, 150 (1969).

⁹S. K. Allison, *Rev. Mod. Phys.* **30**, 1137 (1958).

¹⁰G. Ryding, H. D. Betz, and A. B. Wittkower, *Phys. Rev. Letters* **24**, 123 (1970).

¹¹H. D. Betz and L. Grodzins, *Phys. Rev. Letters* **25**, 211 (1970).

¹²H. D. Betz, *Phys. Rev. Letters* **25**, 903 (1970).

¹³N. Bohr, *Kgl. Danske Videnskab. Selskab, Mat. Fys. Medd.* **18**, No. 8 (1948); N. Bohr and J. Lindhard, *ibid.* **28**, No. 7 (1954).

¹⁴G. I. Bell, *Phys. Rev.* **90**, 548 (1953).

PHYSICAL REVIEW A

VOLUME 3, NUMBER 1

JANUARY 1971

Analysis of the N⁺-Ar and O⁺-Kr Collisions*

H. C. Hayden and E. J. Knystautas†

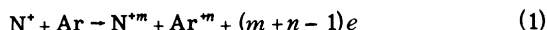
Physics Department, University of Connecticut, Storrs, Connecticut 06268

(Received 11 March 1970)

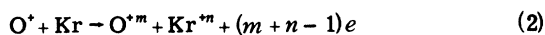
A statistical model, similar to that of Everhart and Kessel, (E-K) is described for N⁺-Ar and O⁺-Kr collisions of the type $X^+ + Y \rightarrow X^{*m} + Y^{*n} + (m+n-1)e$. The E-K model utilizes coincidence data on inelastic energy distributions (usually Gaussian) and average probabilities $\bar{P}_n(\bar{E})$ for n -fold ionization to construct (by an unfolding procedure) intrinsic ionization probabilities $P_n(E)$ for collisions wherein X and Y are of the same species. In the present case of asymmetric collisions, it is necessary to devise a scheme to determine the manner in which the average inelastic energy (\bar{Q}) is divided (into \bar{E}' and \bar{E}'') between the two colliding partners. Three such schemes (shown to be mutually consistent) are presented, one of which assumes that the average inelastic energy associated with an m , n event varies linearly with the spectroscopic energy deficits for the ions in charge states m and n ($\bar{Q}_{mn} = A + BU'_m + CU''_n$), and calculates the required coefficients by a least-squares procedure. Values of \bar{E}'_m and \bar{E}''_n are then calculated from the assumption that the outer shell electrons in the two atoms contribute equally to A . The E-K model is then applied to each atomic species investigated. Statistical assumptions tested are that \bar{E}'_m is independent of n (and \bar{E}''_n is independent of m), and that the intrinsic ionization probabilities depend only upon the inelastic energy E received by the atoms even when the atom collides with one of another species. The probabilities obtained for argon ions in N⁺-Ar collisions agree reasonably well with those obtained for Ar⁺-Ar collisions. The data available on the O⁺-Kr and Kr⁺-Kr reactions are somewhat sparse and preclude a thorough analysis, although the results are encouraging enough to warrant further experimental investigation.

I. INTRODUCTION

We consider here a model for the collision processes



and



at keV energies and large scattering angles. Data for these collisions have recently been published by Knystautas *et al.*¹ The data are of two types: first, the average amount of inelastic energy \bar{Q}_{mn} associated with an (m, n) event; and second, the corresponding average probabilities \bar{P}'_m and \bar{P}''_n , wherein the incident kinetic energy T_0 and laboratory scattering angle θ are specified.

Various models^{2,3} have been developed for symmetric collisions (Ar⁺-Ar, Ne⁺-Ne, Kr⁺-Kr) and more recently for the Ar⁺-Cu collision.⁴ A central assumption in all of these models is originally due

to Russek,² viz., that the probability P_i of removing i electrons from an atom is a function of the inelastic energy E that the atom receives in the collision. The experimental test of this assumption is not trivial because in any choice of collision parameters (T_0, θ, m, n) there is not a single inelastic energy E but rather a distribution in E . The model of Everhart and Kessel³ allows for this distribution and calculates $P_i(E)$ for the symmetric Ar⁺-Ar,³ Ne⁺-Ne,⁵ and Kr⁺-Kr⁶ collisions.

A problem arising in the asymmetric N⁺-Ar and O⁺-Kr collisions considered here is that of evaluating the amount of energy which goes into the inelastic channels of each of the colliding partners. Measurements performed on the energy, momentum, angles of scatter and recoil, etc., easily yield the total average inelastic energy \bar{Q} associated with a collision but are not sufficient to determine how this energy is divided between the two ions.

The consistency method described below shows that the average amount of inelastic energy \bar{E}'_m (\bar{E}''_n)